Optics and Lasers in Engineering 78 (2016) 48–54

Contents lists available at ScienceDirect

Optics and Lasers in Engineering

journal homepage: www.elsevier.com/locate/optlaseng

Subwavelength structures for high power laser antireflection application on fused silica by one-step reactive ion etching

Xin Ye, Xiao-Dong Jiang, Jin Huang, Lai-Xi Sun, Feng Geng, Zao Yi, Xiao-Tao Zu, Wei-Dong Wu, Wanguo Zheng *

Research Center of Laser Fusion, China Academy of Engineering Physics, Mianyang, Sichuan 621900, China

ARTICLE INFO

Article history:
Received 17 July 2015
Received in revised form
8 September 2015
Accepted 2 October 2015
Available online 24 October 2015

Keywords:
Subwavelength structures
Antireflection
Colloidal crystals
Reactive ion etching
Laser induce damage threshold

ABSTRACT

In this paper we report a simple method to fabricate a novel subwavelength structure surface on fused silica substrate using one-step reactive ion etching with two-dimensional polystyrene colloidal crystals as masks. The etching process and the morphologies of the obtained structure are controlled. We show that the period of the obtained fused silica pillar-like arrays were determined by the initial polystyrene nanoparticle size. The height of pillar arrays can be adjusted by controlling the etching duration, which is proved to be of importance in tailoring the antireflection properties of subwavelength structures surface. The novel subwavelength structures surface exhibit excellent broadband antireflection properties, but the size of the pillar affects the antireflective properties in short wavelength region. We anticipate this method would offer a convenient and scalable way for inexpensive and high-efficiency high power laser field designs.

1. Introduction

In the last few decades, steady efforts have been made to achieve broadband antireflection characteristics for various optical components [1–6]. Especially, antireflection technology is currently indispensable for improving the performance for different applications, such as superluminescent diodes (SLEDs) [7–9], flat-panel displays, and solar cells [10]. Some nocturnal insects use arrays of non-close-packed nipples of sub-micrometer size as antireflective structures to reduce reflection from their compound eyes [11]. The antireflective surface with a period shorter than the wavelengths of visible light can suppress the reflection of light. This antireflection effect provided by a microstructure surface is known as a “moth-eye” [12,13], and the antireflective structures surface is called an antireflective subwavelength structures (SWS) surface [14–16]. The current anti-reflective technologies can be broadly divided into two categories [5]: thin film anti-reflective coatings [17–19] and SWS surface [20–23]. Unfortunately, even though antireflection coatings using multilayer thin-film stacks are widely used, there still exist many problems associated with material selection, band limitation, and thermal mismatch between the film and the substrate. The SWS surfaces exhibit distinct advantages compared to coatings. First, the SWS surfaces exhibit higher Laser-induced-damage thresholds [24] and better durability than coatings because no foreign materials are involved when they are used over a high power laser range. Second, the material of the SWS surfaces is the same as that of substrates, while coating materials with appropriate refractive index are rare in nature [1–3]. Last, the SWS surfaces have many tunable factors, such as the spacing, depth and cross-sectional geometry [25,26]. Similar to the nipple arrays in moth eyes, the SWS surfaces with pillar-like profiles exhibit an equation refractive index between air and substrate. Therefore, they can dramatically suppress the reflection losses at the interface [27]. Indeed, SWS surfaces have been used for improved diffractive gratings, diffractive lenses, and antireflection coatings on semiconductor substrates [28–30]. SWS surfaces are commonly produced by top–down technologies, such as interference lithography[31], electron beam lithography[16] and deep-ultraviolet photolithography. For ultraviolet and visible light applications, feature sizes below 200 nm are always necessary. Preparing structures with such a feature size is beyond the conventional photolithography capability. Although deep-ultraviolet photolithography and electron beam lithography achieve the resolution down to nanometer scale, the costs are always very high because of the expensive facilities and the complex preparation procedures. Self-assembly technology provides a much simpler and cheaper alternative in creating sub-micrometer scale periodic arrays[32]. Recently, antireflective surfaces on substrate prepared by nanosphere lithography have been reported [33,34]. However, there are few SWS surfaces on fused silica. In this paper

* Corresponding author. Tel./fax: +86 816 2480830.
E-mail address: yehanwin@mail.ustc.edu.cn (W. Zheng).

http://dx.doi.org/10.1016/j.optlaseng.2015.10.005
0143-8166/

we demonstrate how fused silica nanopillar arrays with antireflective behavior are created based on the combination of self-assembly of polymer spheres into two dimensional (2D) arrays and reactive-ion etching (RIE). We investigate the optical reflectance and transmission spectroscopy of such a fused silica SWS. Scattering resulted in size of the nanostructures in the short wavelength range is demonstrated and elucidated. The laser damage threshold of SWS was carried out on Nd:YAG lasers at 1064 nm.

2. Method

2.1. Synthesis of monodisperse PS

Monodisperse PS was synthesized using an emulsifier-free emulsion polymerization technique [35]. A five neck, round-bottomed flask was filled with water and the washed styrene, removed polymerization inhibitor, and then heated to 80 °C. Attached to the flask was an electric motor driving a glass string rod and Teflon wedge, a thermometer, a condenser, a pipe through which house nitrogen was bubbled to deaerate the mixture, and a stopper for the addition of reactant. Then the hot initiator solution (potassium persulfate) was added into the flask. The temperature was kept at 80 °C while the mixed solution was stirred about 300 rad/min for 24 h. The resulting latex spheres remained suspended in their mother liquor until needed. The concentration can be adjusted by adding deionized water into the mother liquor.

2.2. Assembly of the 2D PS colloidal crystal templates

The PS microsphere monolayers were prepared by dip coating, which was developed from Nagayama's method [36]. Experimental procedures of assembly of the colloidal crystal are as follows: first, a suspension of the particles was diluted to a definite concentration using deionized water. PS particles were modified with Sodium dodecyl sulfate (SDS) so as to terminate them with negative charged groups and prevent aggregation before self-assembly. Then, a hydrophilic fused silica substrate was immersed vertically into the dispersion and lifted up with a constant speed, which was precisely controlled by a motor. The temperature for the experiment was set at 20 ± 2 °C.

2.3. SWS surfaces fabricated by RIE

The SWS surfaces were fabricated by RIE process. The RIE process was using a 10:1 mixture of Ar and CHF_3 as a process gas at a total flow rate of 165 SCCM, chamber pressure 1.2 pa and RF power 100 W. PS spheres are finally removed by tetrahydrofuran for 30 min. Samples were washed with ethanol to generate clean fused silica SWSs.

2.4. Characterization

The diameter of the spheres was estimated using Mastersizer 2000 Laser particle sizer. The morphology of the colloidal crystals template and SWSs were examined using a JSM-7401 scanning electron microscopy (SEM). The samples were sputtered with a thin layer of Au prior to imaging. Transmission and reflection measurements were performed using a Lambda 950 spectrometer (the specular reflection and transmission were measured at an incidence angle of 15°.) The angle-dependent specular transmission was measured by an ultraviolet–visible spectral measurement accessory (Lambda 950 spectrometer) from 300 nm to 1200 nm (at an incidence angle 0°, 15°, 30°, 45°). The LIDT was test with the Q-tuned Nd:YAG laser was used to provide a near-Gauss-type pulse beam (spatially and temporally) at a 1064 nm wavelength. A fixed energy attenuator was installed in the beam path to provide energy control. The maximum output energy was up to 1 J. The diameter of the laser spot on the testing sample was ~1 mm. (the width at $1/e^2$ of the pulse intensity), and the pulse width was ~3 ns. The R-on-1 testing procedure was carried out at 20 locations that were arranged in to a 4×5 array. According to ISO11145, the distance between any two closer irradiated spots was 3 mm, which was long enough to avoid the over lapping of damage regions. By increasing the energy irradiated on the sample at an increment of 0.3 mJ and a time interval of 3 s, the samples were shot until breakdown damage (plasma flash) occurred, and this energy was recorded at once. The final LIDT of SWS and substrate were the root mean square of 20 breakdown damage energies.

3. Result and discussion

A schematic diagram of process steps for fabricating the SWSs surface by monolayer PS colloidal crystals template and RIE on fused silica substrate is shown in Fig. 1. Monodisperse PS particles were produced by an emulsifier-free emulsion polymerization synthesis [35]. First, the dip-coating technique is used to generate colloidal monolayers of hexagonally ordered PS particles on fused silica substrate [37]. Second, fused silica SWS were formed by fluorine based chemistry selective and anisotropic RIE of the fused silica substrate using a mixture of Ar and CHF_3. PS particles protect fused silica immediately underneath them, resulting in the formation of pillar-like arrays directly on fused silica surface. The patterns of the polystyrene spheres were transferred to the fused silica substrates, the period of the nanopillars were determined by the initial nanoparticle size. Finally, The PS particles at the tips of

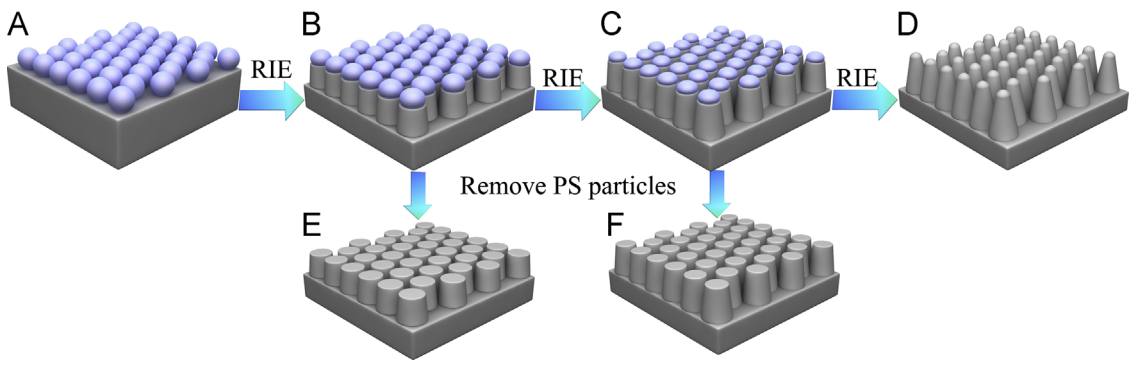

Fig. 1. Schematic of the fabrication procedures for the shape control of nanopillars. (A) PS monolayer colloidal crystals on fused silica substrate; (B) pillar-like arrays with PS on the top; (C) truncated cone arrays with PS on the top; (D) paraboloid-shaped arrays on the fused silica; (E) pillar-like arrays on fused silica; (F) truncated cone arrays on the fused silica.